

Polymer brushes with reversibly tunable grafting density

Leonid I. Klushin

*Department of Physics, American University of Beirut. P. O. Box 11-0236, Beirut 1107 2020, Lebanon and
Institute of Macromolecular Compounds, Russian Academy of Sciences. 31 Bolshoy pr, 199004 Saint Petersburg, Russia*

Alexander M. Skvortsov

Chemical-Pharmaceutical University. Professora Popova 14, 197022 St. Petersburg, Russia

Alexey A. Polotsky and Anna S. Ivanova

Institute of Macromolecular Compounds, Russian Academy of Sciences. 31 Bolshoy pr, 199004 Saint Petersburg, Russia

Friederike Schmid

Institut für Physik, Johannes Gutenberg-Universität Mainz, Staudingerweg 7, D-55099 Mainz, Germany

We propose a novel class of responsive polymer brushes, where the effective grafting density can be controlled by external stimuli. This is achieved by using end-grafted polymer chains that have an affinity to the substrate. For sufficiently strong surface interactions, a fraction of chains condenses into a near-surface layer, while the remaining ones form the outer brush. The dense layer and the more tenuous outer brush can be seen as coexisting microphases. The effective grafting density of the outer brush is controlled by the adsorption strength and can be changed reversibly and in a controlled way as a response to changes in environmental parameters. The effect is demonstrated by numerical SCF calculations and analyzed by scaling arguments. Since the thickness of the denser layer is about a few monomer sizes, its capacity to form a microphase is limited by the product of the brush chain length and the grafting density. We explore the range of chain lengths and grafting densities where the effect is most pronounced. In this range, the SCF studies suggest that individual chains inside the brush show large rapid fluctuations between two states that are separated by only a small free energy barrier. The behavior of the brush as a whole, however, does not reflect these large fluctuations, and the effective grafting density varies smoothly as a function of the control parameters.

I. INTRODUCTION

Polymer brushes are commonly used for permanent surface modification to mediate the stability of colloidal dispersions, provide anti-fouling properties, and protect the system from degradation [1–5]. Brushes can also act as smart stimuli-responsive materials that change surface wetting properties reversibly or act as sensors [6–10].

Under good solvent conditions, the physical properties of brushes are determined by two key parameters: the chain length and the grafting density. Together, they determine the thickness of the brush layer and the strength of the repulsive forces that the brush exerts on objects approaching the surface. In general, both the chain length and the grafting density are set at the stage of the brush synthesis and cannot be changed thereafter. This is also the situation which is considered in most theoretical studies.

The aim of the present paper is to extend this concept. We propose to use brushes formed by end-grafted adsorption-active chains, in which case properties are affected by the short-range adsorption interactions between the substrate and the chain units. The properties of such brushes are studied by self-consistent field (SCF) calculations and a scaling analysis. We predict that over a wide range of adsorption strengths, part of the brush chains are almost completely laid out on the surface while the remaining chains form a brush with a reduced grafting

density. Hence it is possible to reversibly control the effective brush grafting density and, therefore, its properties, by changing the strength of the adsorption potential. Experimentally, the adsorption strength can be changed in two ways: 1) by changing the composition of a mixed solvent (this can result in a very strong variation of the adsorption parameter), and 2) by changing the temperature of a mixed solvent which would result in a finer tuning). A large array of mixed solvents adjusted for specific polymer-substrate pairs was developed in the context of liquid chromatography studies [11]

A brush is often considered as a semi-dilute polymer system; it is natural to expect some similarities between the behavior of the brush composed by adsorption-active chains and the adsorption from a semi-dilute solution. In both cases, the attraction to the substrate competes with a local accumulation of monomers leading to an increase in steric repulsion and eventually to saturation. In the case of adsorption from solution, bound chains form a dense proximal layer whereby they are in contact with the substrate, but also a tenuous more distant layer composed by tails [12]. In the case of adsorption-active brushes a new factor comes into play: All chains are permanently attached to the surface even when they are not bound by adsorption. Hence, two scenarios are conceivable: 1) a part of each chain starting from the grafted end is adsorbed while the rest of the chain forms a tail, and 2) a certain fraction of chains is fully adsorbed, and the

remaining ones are desorbed and form the outer brush. We demonstrate below that the second scenario applies.

II. MODEL AND METHOD

We consider a polymer monodisperse brush made of linear flexible macromolecules grafted at one end onto a solid planar substrate. A polymer chain is composed of N identical monomer units, the chains are grafted onto the surface at the grafting density σ , defined as the number of grafted polymer chains per unit surface area. The surface is assumed to be attractive to all polymer chains, the monomer-surface attraction is characterized by the adsorption energy $-\varepsilon$, $\varepsilon > 0$. The brush is immersed into an athermal solvent; in terms of Flory-Huggins interaction parameter χ this corresponds to $\chi = 0$. To calculate the system's partition function and its various properties, we use the Scheutjens–Fleer self-consistent field (SF-SCF) method. The SF-SCF method and its modifications for the study of polymer brushes of various types have been repeatedly described in the literature and can be found, for example, in [12]. The SF-SCF approach uses a lattice, which facilitates to account for the volume of all molecular components, and also takes into account the symmetry of the problem under consideration. Polymer chains are, therefore modeled as walks on the simple cubic lattice. The lattice cell size is equal to the size of a monomer unit, each lattice site can be occupied either by a monomer unit by or a solvent molecule. The lattice sites are organized in a planar layers, each layer is referred to with a coordinate z normal to the grafting plane. Within a layer with fixed z , i.e. along x and y axes, the volume fractions of the monomeric components and the self-consistent potential are taken as uniform; hence, we use a one-gradient version of the SF-SCF method for planar geometry. A monomer unit in the first lattice layer adjacent to the surface has a contact with the surface and acquires an additional energy gain $-\varepsilon$. More details about the implementation of the SF-SCF method is given in Appendix A. In order to obtain a physical understanding of the effects observed in the SCF calculations and characterize the crossover between different regimes, we complement them with a scaling analysis using "blob" concepts as outlined in Refs. [13, 14].

Throughout this paper, energies are given in units of $k_B T$ and lengths in units of the statistical segment length or monomer size a , corresponding to the lattice cell size in the Scheutjens-Fleer method.

III. RESULTS OF THE SCF CALCULATIONS

A. Adsorption regimes in the brush

As the monomer-substrate attraction strength changes, the brush undergoes a certain restructuring. The brush thickness can be characterized by the average

height of the free ends, $\langle z_e \rangle$, which decreases monotonically with an increase in the adsorption parameter, ε , as demonstrated in Figure 1. A saturation effect at large values, $\varepsilon \gtrsim 3$, is due to complete filling of the first layer by the adsorbed monomers. The larger the area per chain, $1/\sigma$, the stronger the brush thickness is affected by the attraction to the substrate. When the surface is able to bind all the monomers, at sufficiently strong adsorption the brush thickness reduces to one monomer length independently of the chain length. Strictly speaking, these fully adsorbed states could be laterally inhomogeneous if $1/\sigma$ is much larger than the squared lateral size $R_{lat}^2 \propto N^{3/2}$ of the effectively 2-dimensional adsorbed coil. However, the one-gradient version of the SCF method does not allow to resolve lateral inhomogeneity and is more suited to describe configurations when the z -profile of the monomer density is formed by several overlapping chains.

Figure 2 displays the N -dependence of the brush thickness in the saturation regime ($\varepsilon = 5$) for several values of the grafting density. Brushes composed of short chains are completely adsorbed: no residual brush is left in the saturation regime. Brushes composed of chains longer than a certain characteristic value, $N^*(\sigma)$, cannot be fully adsorbed as the number of monomers per unit area exceeds the adsorption capacity of the substrate. Hence, even in the saturation limit, the surface retains non-adsorbed chain tails, leading to an (approximately linear) increase in the brush thickness with N . We will refer to these two saturation limits as to the "bald" and "hairy" regimes. The inset shows that the characteristic chain length separating the completely adsorbed and the partially adsorbed regimes (red circles) satisfies the relation $N^*\sigma \approx 1$, so that the area per chain, $1/\sigma$, is approximately equal to N . The condition $(\sigma N)^* = 1$ marks a crossover point between regimes, which can be crossed both by varying the chain length N at fixed grafting density σ , or by varying σ at fixed N . Just from looking at Figs. 1 and 2, the nature of the partially adsorbed state is not yet clear. Two scenarios are conceivable: In the first one (Scenario 1), all chains are partly adsorbed and contain fN adsorbed monomers and desorbed tails of length $N(1-f)$. In this case, the desorbed tails (the hairs) form an outer brush with effective grafting density σ and effective chain length $N_{eff} = N(1-f)$. In the second scenario (Scenario 2), a fraction q of chains is fully adsorbed, and the remaining ones are fully desorbed and form the outer brush. The effective grafting density of the outer brush is then reduced, $\sigma_{eff} = \sigma(1-q)$, and the effective chain length is given by N . Below, we will show that this second scenario applies in our system.

Due to the limitation of the SCF method, we also cannot tell immediately whether the "hairy" state in the saturation limit involves a well-formed residual brush or the non-adsorbed tails form isolated "mushrooms". In order to address this question, we compare the average free end height, $\langle z_e \rangle$ obtained from the SCF calculations with the analytical result $\langle z_{coil} \rangle = \sqrt{\pi N/6}$ for an iso-

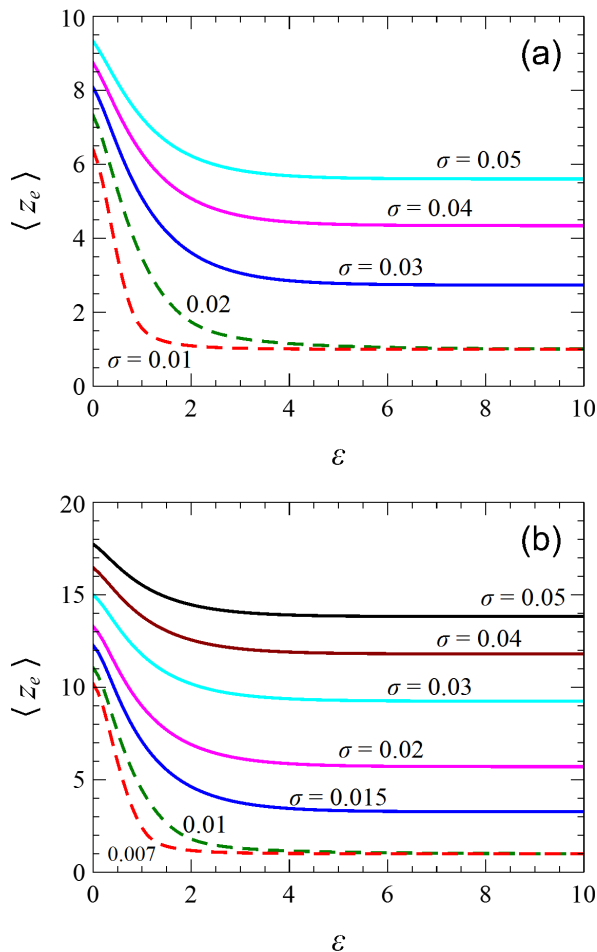


Figure 1. Average distance of the free chain's ends from the grafting surface in a monodisperse brush made of polymer chains with $N = 50$ (a) and $N = 100$ (b) monomer units grafted at the density σ (indicated) as a function of the polymer-surface adsorption energy ε . Solid and dashed curves correspond to “hairy” and “bald” regimes, respectively.

lated ideal coil of length N grafted at the impenetrable substrate. Hereafter, we use the criterion $\langle z_e \rangle = \langle z_{coil} \rangle$ to identify the boundary between the residual brush and mushroom regimes. This boundary is shown in the inset of Figure 2 (blue squares) and is well described by the condition $(N\sigma)^* \approx 2.5$. In the rest of the paper we will focus on the regimes where the residual brush exists at any adsorption strength, $N\sigma > 2.5$. A study of the other regimes at smaller grafting densities would require a method allowing the resolution of laterally inhomogeneous structures.

B. Self-consistent profiles of densities and fields

The monomer density profiles change gradually with the increase in the adsorption parameter, ε , as demonstrated in Figure 3. A denser layer is formed in the near-

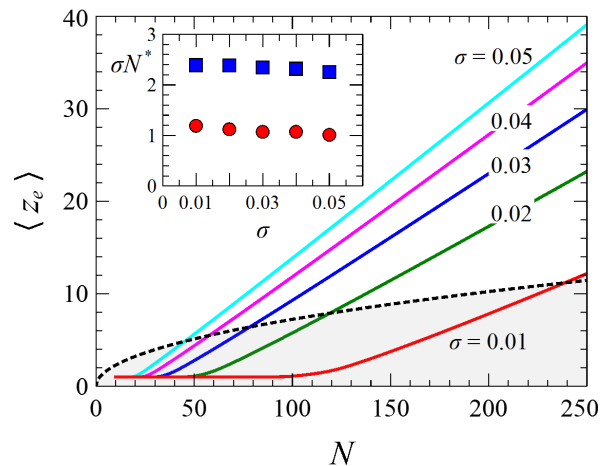


Figure 2. Average distance of the free chain's ends from the grafting surface in the saturation regime ($\varepsilon = 5$) as a function of the chain length, N , for several values of the grafting density σ (indicated in the figure). Black dashed line shows the boundary $z = \sqrt{\pi N/6}$ between the mushroom and brush regimes. Inset: the crossover values of the product $(\sigma N)^* \approx 1$ separating the “bald”, $\sigma N < 1$, and the “hairy”, $\sigma N > 1$, regimes (red circles) and mushroom and brush regimes (blue squares) are both essentially independent of the brush grafting density, σ .

est vicinity of the grafting surface. The residual brush becomes thinner in terms of its z -extension and simultaneously shows a decrease in monomer density (except for the adsorbed layer). In an inert brush with an intermediate density adequately described by the mean field in the second virial approximation, the density profile coincides with the potential of the mean force, $u(z) = v\varphi(z)$ where v is the excluded volume parameter taken as $v=1$ in the present study. The asymptotic shape of this field for well-formed brushes is given by a well-known parabolic formula [15, 16] $u(z) = \frac{3}{2} \left(\frac{\pi}{2} \sigma v \right)^{2/3} - \frac{3\pi^2}{8N^2} z^2$. Note, however, that the analytical expression does not describe the drop in the field in the closest vicinity to the substrate which exists at $\varepsilon = 0$ and is important in the context of adsorption, see Figure 3b. With increasing adsorption strength the density near the substrate increases and eventually approaches dense packing. Clearly, the second virial approximation is no longer valid and in the numerical SCF scheme, the Flory expression relating the effective field to the local density, $u(z) = -\log[1 - \varphi(z)]$, is used. Importantly, the shape of the potential stabilizes at large values of the adsorption parameter (in the saturation regime), and the limiting shape is shown with $\varepsilon = 7$ by the solid line. Both the attractive well depth and the repulsive peak eventually stop depending on ε as shown in the inset.

Figure 4 displays the monomer density in the first adsorption layer, φ_1 , as a function of the adsorption parameter, ε , for different chain lengths and grafting densities. The curves nearly collapse. The N -dependence is neg-

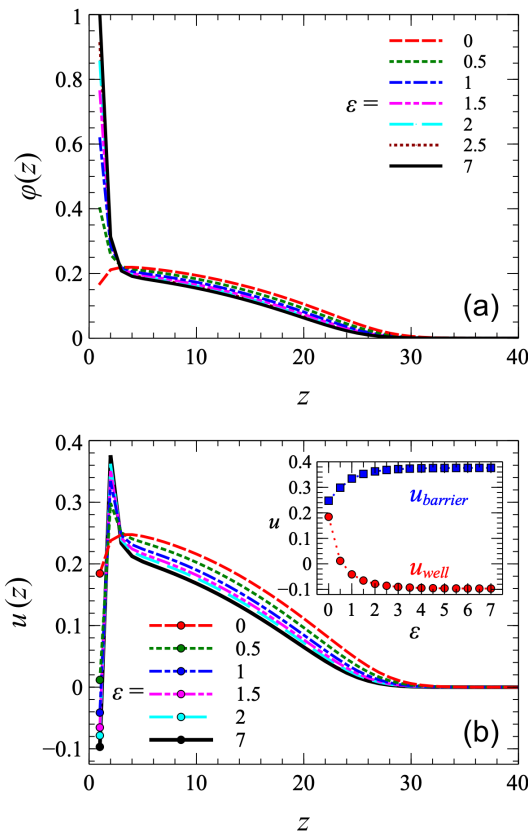


Figure 3. Polymer density profiles, that is, the volume fraction of segments φ as a function of the distance z from the grafting surface (a) and the corresponding self-consistent field potential profiles (b) for a monodisperse brush made of polymer chains with $N = 100$ monomer units grafted at the density $\sigma = 0.04$ at various values of the polymer-surface adsorption energy ε , as indicated. Inset to panel (b) shows the values of the maximum (barrier) and the surface minimum (well) as functions of the adsorption parameter $\varepsilon \geq 0$.

ligible overall, and the dependence on σ appears to be noticeable only at small values of the adsorption parameter. Very qualitatively, the curves resemble those of the Langmuir theory of adsorption with its saturation effect and an approximately exponential approach to the saturation value $\varphi_1 = 1$.

C. Evidence for micro phase separation in the brush

In order to obtain more insight into the adsorption scenarios, we inspect the chain end distributions in the following Figure 5. Figure 5a displays the evolution of the chain end distributions with the increase in the adsorption strength for the case of $N\sigma = 4$. It is clear that for all values of $\varepsilon \geq 0.5$ the distribution is bimodal. Figure 5 suggests that one can identify two coexisting phases, the adsorbed phase with the chain ends local-

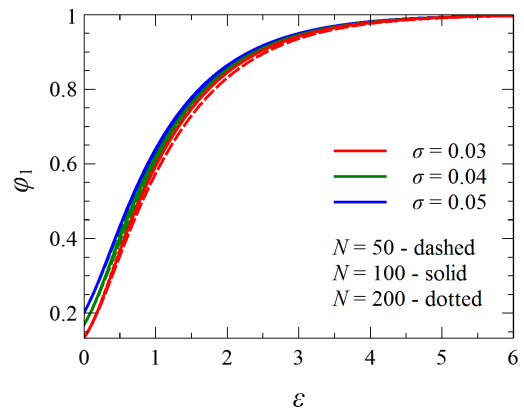


Figure 4. Polymer volume fraction at the surface, that is, in the first adsorption layer $z = 1$, in a monodisperse brush made of polymer chains with $N = 50$ (dashed lines), 100 (solid lines), and 200 (dotted lines) monomer units grafted at the density $\sigma = 0.03$ (red curves), 0.04 (green curves), and 0.05 (blue curves) as a function of the polymer-surface adsorption energy.

ized near the substrate within a few monomers layers, and the brush phase with a broad chain end distribution familiar for the neutral brushes. The maximum describing the adsorbed chains becomes more prominent with increasing ε . This is a clear indication of the adsorption scenario 2 introduced in Section III A: At any given moment, a certain fraction of chains belongs to the localized adsorbed phase with a large number of monomers in contact with the surface, while the other chains form a brush with an effectively reduced grafting density. If the fraction of adsorbed chains is q , the effective grafting density of the residual brush is $\sigma_{\text{eff}} = \sigma(1 - q)$. In scenario 1, all chains would have similar conformations with an adsorbed and desorbed chain block, and the chain end distribution would always be unimodal.

Since in a monodisperse brush all chains are identical, the actual scenario means that chains can fluctuate between two states. Figure 5b shows $-\ln P_e(z)$ which can be interpreted as an effective potential landscape for single chains. The two minima are separated by a very low barrier of no more than $1 k_B T$ (see inset), suggesting that the states are not really well separated and chains fluctuate rapidly between the two, without being trapped in one state for long. Quite unexpectedly, this remains true even when the adsorption parameter ε is increased up to $10 k_B T$ or higher, since the shape of the distribution stabilizes. On the other hand, this effect is in line with de Gennes saturation argument for adsorbed polymer layers whereby the adsorption free energy gain is outbalanced by steric repulsion [17–20].

For a monodisperse brush, the SF-SCF method does not allow to determine the fraction of chains in the adsorbed phase, q , or σ_{eff} directly. Nevertheless, we can suggest a way of determining q or σ_{eff} based on the similarity between the residual brush and a conventional brush

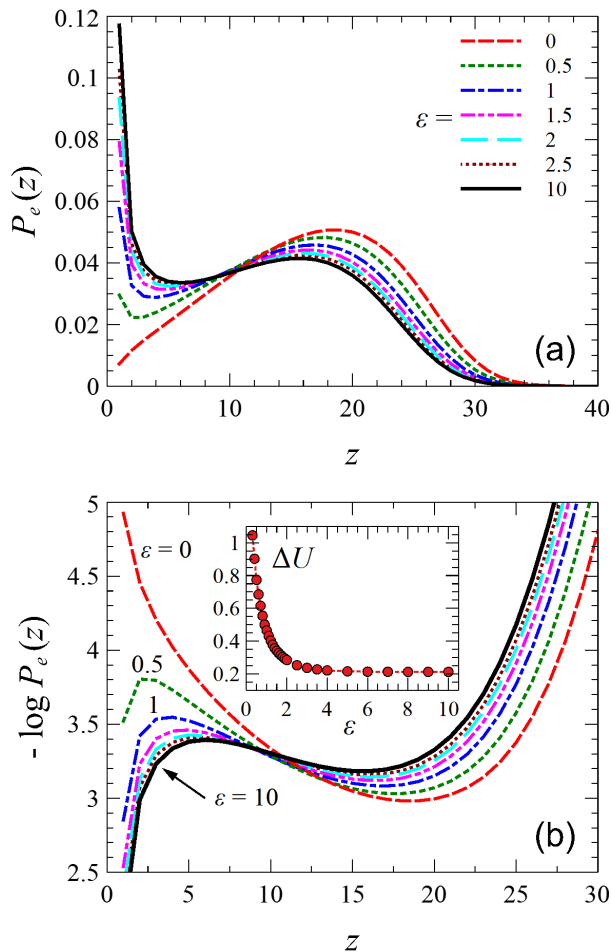


Figure 5. Distributions $P_e(z)$ (a) and the non-equilibrium free energy, $-\log P_e(z)$, (b) for the free ends of brush chains in a monodisperse brush with $N = 100$ and $\sigma = 0.04$ at various polymer-surface adsorption energy ϵ , as indicated. The inset shows the free energy barrier counted from the brush minimum.

grafted onto a non-attractive surface. The procedure is illustrated by Figure 6. Here we show the full density profiles $\varphi(z)$ (panel a) and the density profiles of free ends $\varphi_e(z)$ (panel b) for brushes with $\epsilon = 0.5$ (red curves) and $\epsilon = 3$ (blue curves) grafted at $\sigma = 0.04$ plotted together with those for the non-adsorptive (neutral) brush ($\epsilon = 0$) in the range of $\sigma = 0.02 \dots 0.04$ with $\Delta\sigma = 0.001$ for the sake of better visibility; in the actual fitting procedure we used a 10 times smaller step $\Delta\sigma = 0.0001$.

To extract σ_{eff} , we compare the density profile and ends distributions in a brush grafted the density σ at $\epsilon > 0$ with the profiles obtained for the brush at $\epsilon = 0$ and various grafting densities σ (Figure 6a). We calculate the mean-square distance between two profiles defined as

$$(\Delta\varphi)^2(\sigma_1) = \sum_{z \geq z_0} [\varphi(z, \sigma, \epsilon) - \varphi(z, \sigma_1, 0)]^2 \quad (1)$$

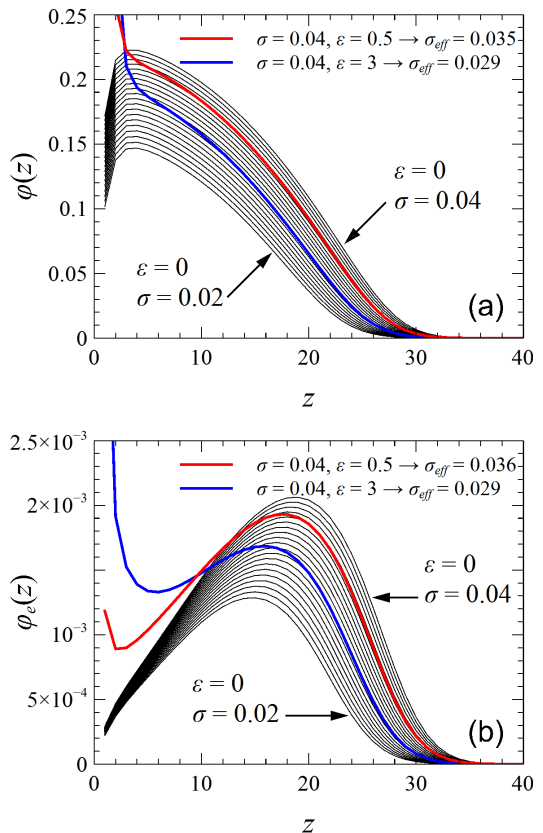


Figure 6. Determination of the effective grafting density of a polymer brush made of polymer chains with $N = 100$ and $\sigma = 0.04$ at the adsorption energy $\epsilon = 0.5$ (red lines) and free ends' density profile (a) and free ends' density profile (b). Thin black lines are the overall polymer density profiles (a) and free ends' density profiles (b) in monodisperse brushes with $N = 100$ and neutral surface ($\epsilon = 0$) and grafting density $\sigma = 0.02, 0.021, 0.022 \dots 0.04$. See explanation in the text

for various values of σ_1 and identify σ_{eff} as the value that minimizes the mean-square distance $(\Delta\varphi)^2$. Here, z_0 is chosen to be the maximum of the end density profile (Fig. 6 b), thus the mean-square distance was only determined in the range of z -values where the neutral brush and the partially adsorbed brush profiles were directly comparable. This procedure was applied both to the full density profiles $\varphi(z)$ and the density profiles of the free ends $\varphi_e(z)$ (Figure 6 a and b).

The dependence of the effective grafting density σ_{eff} determined in this way on the adsorption energy ϵ is shown in Figure 7a. The curves were obtained by fitting the monomer density profiles (solid lines) and the end distributions (dotted lines) and one can see an excellent agreement between these two approaches. With increasing adsorption energy, σ_{eff} monotonically decreases and reaches saturation. In this case, the range of decrease in effective density, $\sigma - \sigma_{\text{eff}}$, is roughly determined by the inverse chain length $1/N$. A basic explanation is pro-

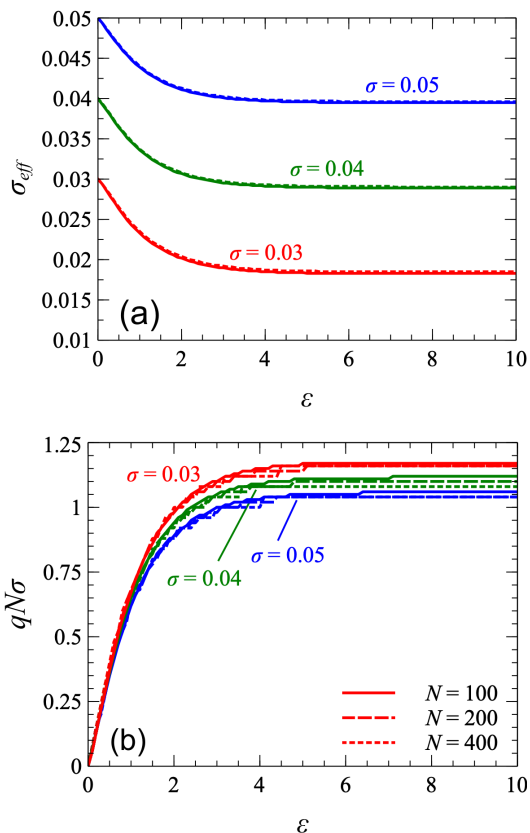


Figure 7. (a) Effective grafting density σ_{eff} in a brush made of polymers with chain length $N = 100$ and different grafting densities σ as indicated. Here σ_{eff} is determined by fitting full monomer density profiles (solid lines) and end density profiles (dashed lines) as described in the main text. (b) Rescaled fraction q of chains in the adsorbed phase as a function of ϵ for different chain lengths N and grafting densities σ as indicated.

vided by the following argument. If we assume that in the saturation regime a chain in the adsorbed phase is completely adsorbed on the surface, then it occupies N lattice cells in the first lattice layer, or the surface area is equal to N . The number of grafted chains per this surface area is $N\sigma$. Hence, the fraction of chains in the adsorbed phase in the saturation regime, $q = 1 - \sigma_{\text{eff}}/\sigma$, is equal to $q^* = 1/(N\sigma)$, and the effective grafting density is thus $\sigma_{\text{eff}} = \sigma(1 - q^*) = \sigma - 1/N$. To test this argument, we show in Figure 7b the rescaled fraction of adsorbed chains, $qN\sigma$, as a function of adsorption strength ϵ for various chain lengths N and grafting densities σ . As expected, it initially grows with ϵ and then saturates at a value close to 1. However, the saturation value is found to exceed 1, especially for smaller σ . This would imply that the fraction of chain contacts with the surface in the adsorbed phase is smaller than unity.

The average fraction of adsorbed units per chain in the brush as a whole is given by $\langle \theta \rangle = \varphi_1/(N\sigma)$ where $\varphi_1 = \varphi(1, \sigma, \epsilon)$ is the monomer density in the first layer

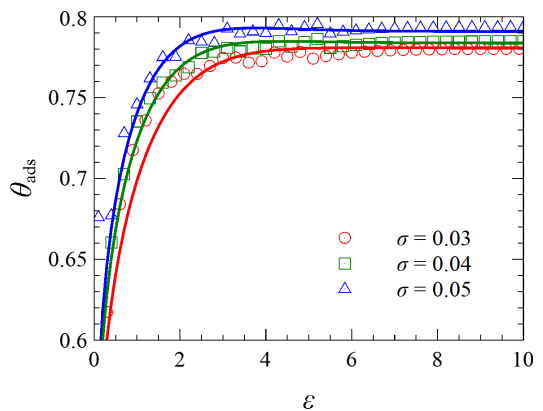


Figure 8. Fraction of contacts in a chain belonging to the adsorbed phase, θ_{ads} , as a function of the adsorption parameter ϵ in a monodisperse polymer brush with $N = 100$ grafted at the density σ as indicated. Symbols show the result of direct calculation of θ_{ads} according to Eq. 2 with the values of $\varphi(1, \sigma, \epsilon)$, $\varphi(1, \sigma_{\text{eff}}, 0)$, and q obtained by the minimization procedure described in the text. Solid curves are obtained with the help of phenomenological fitting for $q(\epsilon)$ and $\varphi(1, \sigma, \epsilon) - \varphi(1, \sigma_{\text{eff}}, 0)$.

$z = 1$. To obtain the fraction of adsorbed units for a chain in the adsorbed phase, θ_{ads} , we should take into account only the fraction of chains in the adsorbed phase q and eliminate the contribution of monomers that belong to chains in the residual brush but are still in contact with the substrate. Then the fraction of monomer-surface contacts in an adsorbed chain is given by

$$\theta_{\text{ads}} = \frac{\varphi(1, \sigma, \epsilon) - \varphi(1, \sigma_{\text{eff}}, 0)}{N\sigma q}. \quad (2)$$

Figure 8 shows the dependence of θ_{ads} on the adsorption energy ϵ calculated according to Eq. (2) using the data presented in . 4 and 7. The symbols are the result of direct application of Eq. (2) to the data points for $\varphi(z = 1, \sigma)$, $\varphi_{\epsilon=0}(1, \sigma_{\text{eff}})$, and q . We have also approximated $q(\epsilon)$ and $\varphi(1, \sigma, \epsilon) - \varphi(1, \sigma_{\text{eff}}, 0)$ by simple phenomenological functions to obtain the curves shown in Figure 8 by solid lines.

The dependence of the fraction of contacts in adsorbed chains θ_{ads} on the adsorption energy ϵ at various grafting densities σ shown in Figure 8 demonstrate that θ_{ads} increases with increasing ϵ reaching a plateau value, which is less than one. This indicates that the chains in the adsorbed phase are not fully adsorbed, even in the saturation regime, and have a small fraction of non-adsorbed units forming loops and tails. The fraction of contacts in adsorbed chains also weakly increases with increasing grafting density. It is also worth noting that already at rather small values $\epsilon = 0.2 - 0.3$ the fraction of contacts in the adsorbed chains is high: $\theta_{\text{ads}} \approx 0.6$.

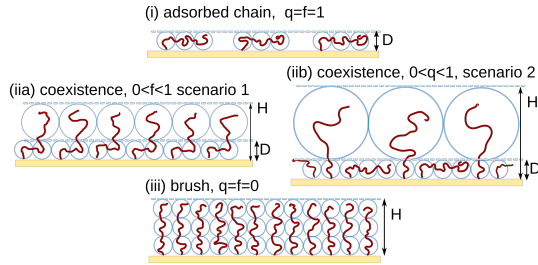


Figure 9. Cartoon showing different regimes in the adsorbing brush. See text for explanation.

IV. SCALING ANALYSIS

In order to obtain more physical insight in the nature of the partially adsorbed state, we will now present a scaling analysis of the system, where we combine blob concepts for adsorbing chains and of polymer brushes [13, 14, 21]. As before, we consider a monodisperse brush made of chains of length N in good solvent, grafted with density σ on an adsorbing substrate with adsorption strength ε . Depending on the chain length and the grafting density we distinguish between different regimes as described in Sec. III A. We will also discuss the two possible scenarios of partial adsorption introduced in Sec. III A.

A. Scaling regimes

1. Regime (i) – Low grafting densities

At very low grafting densities, the grafted chains do not interact with each other and they behave like isolated adsorbing chains.

We begin with briefly recapitulating the simplest scaling picture for a single adsorbed chain [14]. The chain is pictured as a chain of blobs lying on the surface. Every blob has the size D (in units of a) and contains $m \sim D^{1/\nu}$ monomers, where $\nu \approx 3/5$ is the Flory exponent. Thus, the total chain has N/m blobs. According to the blob picture, every blob carries an entropic free energy penalty $k_B T$ to the free energy, resulting in a total entropic contribution $F_e \sim N/m \sim ND^{-1/\nu}$ (in units of $k_B T$). On the other hand, the fraction of monomers in contact with the surface is estimated as $D^{(\phi-1)/\nu}$ [20, 22] and the energy gain due to adsorption is hence given by $F_a \sim -\varepsilon N D^{(\phi-1)/\nu}$, where ϕ is the crossover exponent. The value of ϕ is still debated in the literature. Below, we will approximate it with $\phi \approx 1/2$ which is close to the values obtained from numerical simulations [23–25]. Taking everything together, the total energy is estimated as

$$F \sim ND^{-1/\nu} + \varepsilon N D^{(\phi-1)/\nu} \quad (3)$$

Minimizing this expression with respect to D , we obtain

$$D \sim \varepsilon^{-\nu/\phi} \sim \varepsilon^{-6/5} \quad (4)$$

The chain can be considered adsorbed if it contains several adsorption blobs ($N/m \gg 1$), which implies

$$ND^{-1/\nu} \sim N\varepsilon^{1/\phi} \sim N\varepsilon^2 \gg 1 \quad (5)$$

The total area covered by the chain on the substrate is estimated as

$$A_c \sim N/m D^2 \sim N\varepsilon^{(1-2\nu)/\phi} \sim N\varepsilon^{-2/5} \quad (6)$$

As the grafting density σ increases, the adsorbed chains start to interact and the two dimensional blob chain conformations on the surface influence each other. A detailed scaling analysis of this regime has been carried out by Descas *et al* [20]. Eventually, the surface is fully covered by adsorption blobs and saturates. The crossover to the oversaturated regime is reached at $\sigma A_c \sim 1$ (where A_c is given by Eq. (6)), hence [20]

$$(\sigma N)^* \sim \varepsilon^{(2\nu-1)/\phi} \sim \varepsilon^{2/5} \quad (7)$$

2. Regime (ii) – Intermediate grafting densities

Once the overlap concentration is reached, one of the two possible scenarios of partial adsorption discussed in Sec. III A applies. We will discuss them one after the other.

In Scenario 1 (iia in Fig. 9), a fraction f of monomers in each chain adsorbs to the substrate. The remaining tails comprising $N(1-f)$ monomers desorb and together form an outer brush. In the blob picture, the substrate is thus covered by a dense layer of small adsorbed blobs of size D containing m monomers each, covered by a more tenuous layer of larger blobs of size $\sigma^{-1/2}$. The fraction f of adsorbed monomers is estimated as follows: The number of surface blobs per area is given by $(1/D)^2 = \sigma f N/m$. Inserting $m \sim D^{1/\nu}$, one obtains

$$D \sim (\sigma f N)^{-\frac{\nu}{2\nu-1}} \sim (\sigma f N)^{-3} \quad (8)$$

and the adsorption energy per chain $F_a \sim -\varepsilon \sigma f N D^{(\phi-1)/\nu} \sim -\varepsilon (\sigma f N)^{\frac{2\nu-\phi}{2\nu-1}}$. The entropy cost per area is given by the total number of blobs per area, which includes surface (adsorption) blobs and outer brush blobs. The number of adsorption blobs is given by $(1/D)^2 \sim (\sigma f N)^{\frac{2\nu}{2\nu-1}}$. The number of brush blobs in the outer layer corresponds to that of an Alexander brush with grafting density σ and effective chain length $N(1-f)$ and is hence given by [13] $N(1-f)\sigma^{\frac{2\nu+1}{2\nu}}$. Taking everything together, one gets the free energy

$$F \sim -\varepsilon (\sigma f N)^{\frac{2\nu-\phi}{2\nu-1}} + (\sigma f N)^{\frac{2\nu}{2\nu-1}} + N(1-f)\sigma^{\frac{2\nu+1}{2\nu}} \quad (9)$$

In the limit $N \rightarrow \infty$, the last term becomes negligible compared to the first two terms, and it suffices to minimize $F \sim -\varepsilon (\sigma f N)^{\frac{2\nu-\phi}{2\nu-1}} + (\sigma f N)^{\frac{2\nu}{2\nu-1}}$, which results in

$$(\sigma f N) \sim \varepsilon^{(2\nu-1)\phi} \sim (\sigma N)^*, \quad (10)$$

where $(\sigma N)^*$ is the crossover parameter (7) that separates regime (i) and (ii).

In Scenario 2 (ii b in Fig. 9), a fraction q of chains remain fully adsorbed, whereas the remaining chains desorb fully and have no contacts to the surface. The resulting picture is similar to Scenario 1 in many respects. The surface is still first covered by a dense layer of adsorbed small blobs (thickness D), followed by a dilute layer of large blobs, which now have the size $[(1-q)\sigma]^{-1/2}$. The number of surface blobs per area is now given by $(1/D)^2 = \sigma q N/m + \sigma(1-q)$. In the limit of large N , the second term can be neglected. Using $m \sim D^{1/\nu}$, we obtain

$$D \sim (\sigma q N)^{-\frac{\nu}{2\nu-1}} \sim (\sigma q N)^{-3}, \quad (11)$$

which has the same form than Eq. (8) with f replaced by q . Accordingly, the adsorption energy per chain is $F_a \sim -\varepsilon(\sigma q N)^{\frac{2\nu-\phi}{2\nu-1}}$ and the number of adsorption blobs is $(1/D)^2 \sim (\sigma q N)^{\frac{2\nu}{2\nu-1}}$. The number of blobs in the outer layer is that of a regular brush with effective grafting density σq and chain length N , resulting in $N[(1-q)\sigma]^{\frac{2\nu+1}{2\nu}}$. Thus the total free energy is estimated as

$$F \sim -\varepsilon(\sigma q N)^{\frac{2\nu-\phi}{2\nu-1}} + (\sigma q N)^{\frac{2\nu}{2\nu-1}} + N[(1-q)\sigma]^{\frac{2\nu+1}{2\nu}}, \quad (12)$$

which has the same form than Eq. (9) with f replaced by q , except for the last term. However, the last term again vanishes in the limit $N \rightarrow \infty$ in relation to the other two, and can be neglected. Thus the remaining calculation is the same as in scenario 1 (iia in Fig. 9), and one obtains

$$(\sigma q N) \sim \varepsilon^{(2\nu-1)/\phi} \sim (\sigma N)^*. \quad (13)$$

Here, $(\sigma N)^*$ is again the parameter characterizing the crossover from regime (i) and (ii) (Eq. (7)).

Comparing the final free energies in Scenario 1 and Scenario 2, we find that they only differ in the free energy contribution of the outer brush, which is given by $N(1-f)\sigma^{\frac{2\nu+1}{2\nu}}$ in Scenario 1 and by $N[\sigma(1-q)]^{\frac{2\nu+1}{2\nu}}$ in Scenario 2. According to Eqs. (10) and (13), we have $f = q$. From $0 < (1-f) = (1-q) < 1$, we get $(1-q)^{\frac{2\nu+1}{2\nu}} < (1-f)$, hence Scenario 2 is predicted to be more favorable than Scenario 1 in agreement with the SCF results.

An important result from the scaling analysis is that the thickness of the surface layer is independent of σ (in both scenarios). The grafting density of chains in the adsorbed state remains constant and corresponds to the crossover grafting density, $\sigma q \sim \sigma^*$. Setting $q = 1$ in Eq. (13), one recovers the expression Eq. (7) for the crossover grafting density σ^* .

3. Regime (iii) – High grafting densities

At high grafting densities, all chains are fully desorbed. The transition to this state takes place at the grafting

density where the blob size of a pure brush equals the size of the adsorption blob, $\sigma^{-1/2} = D \sim \varepsilon^{-\nu/\phi}$. This second crossover grafting density is thus given by

$$\sigma_0 \sim \varepsilon^{2\nu/\phi} \sim \varepsilon^{12/5} \quad (14)$$

As a consistency check, we can insert this value in the expression for q in Eq. (13) and obtain $q \sim 1/(N\varepsilon^{1/\phi}) \ll 1$ where the last inequality results from Eq. (5). Hence $q \approx 0$ at the transition as it should. Note that the scaling approach is limited to smaller values of ε when a single adsorption blob comprises at least a few monomers.

B. Comparison with SCF results

Based on the results from the previous section, we can now compare the predictions of the scaling analysis with the results from the SCF calculations.

First, we remark that the full series of transitions from (i) *adsorbed* via (ii) *partially adsorbed* to (iii) *desorbed* discussed above can only be observed if σ or ε are varied, but not if N is varied at fixed σ and ε . In the latter case, the phase behavior depends on the value of $x := \varepsilon\sigma^{-\phi/2\nu} \sim \varepsilon\sigma^{-5/12}$. If $x \ll 1$ (weak adsorption), the chains never adsorb, and the grafted polymer layer undergoes a regular transition from a mushroom to a brush with increasing N . If $x \gg 1$ (strong adsorption), the surface is always covered by an adsorbed layer. Upon increasing N in that case, one expects a transition from (i) (fully adsorbed layer), to (ii) (partially adsorbed layer), but the pure brush state is never reached. This situation is studied in Fig. 2. The height of the brush as a function of chain length is expected to behave as

$$H \sim \begin{cases} D \sim \varepsilon^{-6/5} & : N < N^* \sim \varepsilon^{2/5}/\sigma \\ N[\sigma - \sigma^*]^{1/3} & : N > N^* \end{cases}, \quad (15)$$

which explains the crossover from constant to linear behavior as a function of N observed in Fig. 2. The scaling theory predicts the transition point to be independent of σ , $(\sigma N)^* \sim \varepsilon^{2/5}$, in agreement with the SCF results.

When varying ε at fixed σ and N , the scaling theory predicts the regime of partial adsorption to be very broad in the limit of large N , ranging from $\varepsilon_0 \sim \sigma^{5/12}$ to $\varepsilon^* \sim (\sigma N)^{5/2}$. This is confirmed by the SCF results, e.g., Figs. 4, 7, and 8, where the transition to the pure brush cannot be clearly localized.

The fraction of adsorbed chains is predicted to scale as $q \sim \frac{1}{\sigma N} \varepsilon^{2/5}$, which is consistent with the SCF data in Fig. 7. In particular, the data for $q\sigma N$ for different σ and N as a function of ε roughly collapse as predicted (see Fig. 7 b)).

In other respect, the comparison between the SCF results and the scaling theory is only partly convincing. For example, the density of adsorbed contacts $N\sigma q D^{(\phi-1)/\nu} \sim \varepsilon^{7/5}$ is predicted to be independent of N and σ , which is in agreement with the SCF results.

However, the predicted dependence $\sim \varepsilon^{7/5}$ is not reflected in the data of Fig. 4. Likewise, the fraction of contacts in the adsorbed phase is predicted to be $\theta_{\text{ads}} \sim D^{(\phi-1)/\nu} \sim \varepsilon^{(1-\phi)/\phi} \sim \varepsilon$, independent of σ . The corresponding SCF data also seem to roughly collapse for different σ according to Fig. 8. However, the data do not reflect the scaling law $\sim \varepsilon$.

Thus the results of the scaling analysis do qualitatively agree with the SCF results, however, the actual dependence of various quantities on ε is poorly captured. One likely explanation is that the fraction of adsorbed monomers and the size of the adsorption blob saturate at high ε . Indeed, looking at Fig. 3, one gets the impression that the thickness of the adsorbed layer approaches a constant for $\varepsilon > 0.5$ and that this constant is of the order of the lattice constant a .

We can take such saturation effects into account by assuming that the thickness of the adsorbed layer is a general function $D(\varepsilon)$, which has the initial behavior $D \sim \varepsilon^{-6/5}$, but saturates at a constant \bar{D} at large ε . Likewise, we assume that the surface coverage by an adsorbed chain behaves like $A_c \sim N/g(\varepsilon)$, where $g(\varepsilon) \sim \varepsilon^{2/5}$ for $\varepsilon \rightarrow 0$, and $g(\varepsilon) \rightarrow \bar{g}$ at large ε . The relation $\sigma q = \sigma^*$ is taken to be still valid in the saturation regime, i.e., the thickness of the adsorbed sublayer is constant throughout the partially adsorbed regime (ii). Repeating the analysis of Section IV, we obtain similar results, except that the crossover points from (i) to (ii) and from (ii) to (iii) are now given by

$$(\sigma N/g(\varepsilon))^* \sim 1 \quad \text{and} \quad (\sigma D(\varepsilon))_0 \sim 1. \quad (16)$$

Regarding the comparison of the theoretical predictions with the SCF calculations, we find that most of our previous conclusions still hold: At fixed sufficiently large ε and σ , the height of the brush as a function of N still exhibits the crossover from constant to linear behavior

$$H \sim \begin{cases} D \sim \varepsilon^{-6/5} & : N < N^* \sim \varepsilon^{2/5}/\sigma \\ N[\sigma - \sigma^*]^{1/3} & : N > N^* \end{cases}, \quad (17)$$

with a transition point $(\sigma N)^* \sim g(\varepsilon)$ that is independent of σ . The regime of partial adsorption is even wider than before: In fact, when increasing ε for large N , the transition (ii)-(iii) can no longer take place if $\bar{g} < \sigma N$. The rescaled fraction of adsorbed chains, $q\sigma N \sim g(\varepsilon)$ is still predicted to collapse for different σ and N . Also, the density of adsorbed contacts $N\sigma f \frac{1}{\bar{D}} \sim g(\varepsilon)/D(\varepsilon)$ and the fraction of contacts in the adsorbed phase $\theta_{\text{ads}} 1/D(\varepsilon)$ are still independent of N and σ . Both curves are now predicted to rise and saturate at \bar{g}/\bar{D} and $1/\bar{D}$, respectively, in agreement with the SCF data. In particular, the data for θ_{ads} in Fig. 8 suggest that $D(\varepsilon)$ saturates quickly already at $\varepsilon \sim 3$, in agreement with Fig. 3.

V. PHASE TRANSITIONS OF SINGLE "PROBE" CHAINS IN THE BRUSH

It is commonly understood that polymer adsorption involves a phase transition. An isolated chain on a planar substrate undergoes a continuous phase transition (which is smoothed out by finite size effects) and one can identify the critical (or, more precisely, multicritical) adsorption point in the $N \rightarrow \infty$ limit [26, 27]. A minority adsorption-active chain inserted in a neutral brush undergoes a much sharper first-order-like transition where the transition point is affected by the brush density and the relative lengths of the minority and majority chains [7, 28, 29]. In the case of the monodisperse brush where all the chains are adsorption-active we encounter a strange and counter-intuitive picture. On the one hand, we have identified microphase separated states which suggests phase coexistence and some underlying first-order transition. On the other hand, we see that all the characteristics of the brush as a whole as well as of individual chains change quite smoothly with increasing adsorption strength, ε . Phase coexistence is normally expected to be confined to a line in the pressure-temperature plane. In our situation, the brush is not loaded, which corresponds to a fixed zero osmotic pressure. The temperature is associated with the adsorption parameter, but contrary to naive expectations of a transition point, we observe coexistence in a broad range of values of ε . In order to analyze this situation in more detail we show in Figure 3b how the total self-consistent field (including attraction to the surface) changes with the increase in the adsorption parameter. The field profile includes the attractive well of the width of one layer and a broad weakly repulsive barrier. The depth of the attractive well changes very little and remains in the range of 0.2-0.4 $k_B T$ when ε increases from 0.4 to 10 $k_B T$, see the inset in Fig 3b. Simultaneously, the repulsive barrier is also slightly adjusted. This delicate adjustment allows to maintain the broad bi-modal distribution of the free end reflecting a conformation that fluctuates between two phases, as demonstrated earlier in Figure 5.

To gain more insight into this intriguing system we consider a virtual probe chain that differs from all the other brush chains only by its affinity to the substrate which is taken as a new independent parameter, $\varepsilon_{\text{probe}}$. We fix all the brush parameters such as N, σ, ε , and study the properties of the probe chain exposed to the fixed brush potential, as a function of its own adsorption parameter $\varepsilon_{\text{probe}}$. The average fraction of the adsorbed monomers in the probe chain, $\theta(\varepsilon_{\text{probe}})$ is shown in Figure 10a.

The average fraction of the adsorbed monomers in the probe chain, $\theta(\varepsilon_{\text{probe}})$ is shown in Figure 10a. It is clear that for strong enough attraction of the brush chains, $\varepsilon \geq 0.5$, the number of contacts of the probe chain sharply increases when its affinity parameter matches that of the brush itself, $\varepsilon_{\text{probe}} \simeq \varepsilon$. The sharpness of the transition as quantified by the peak value of the reduced mean-

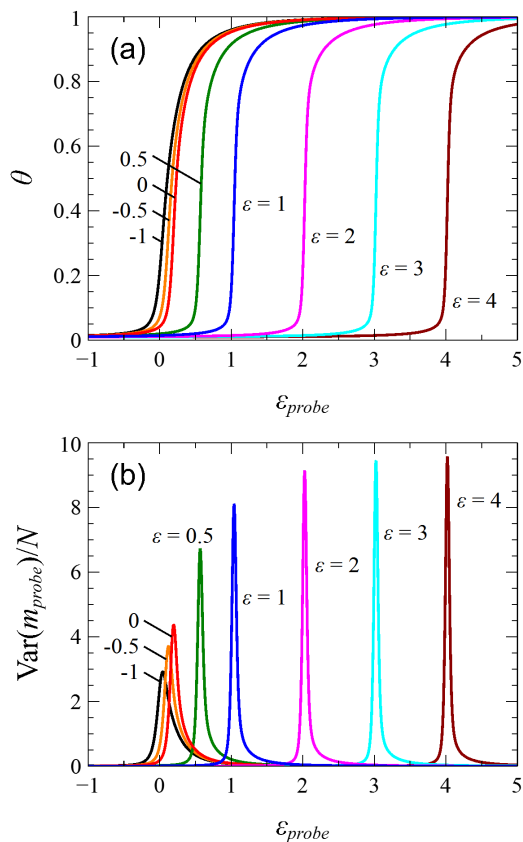


Figure 10. Average fraction of adsorbed units in the probe chain (a) and its variance (b) as function of the probe chain interaction energy ε_{probe} at various brush chains interaction energy ε , as indicated. The probe chain is inserted in the brush with $N = 100$ and $\sigma = 0.04$. The probe chain length is equal to the brush chain length.

square fluctuations, $\text{Var}(m)/N = (\langle m^2 \rangle - \langle m \rangle^2)/N = d\theta/d\varepsilon_{probe}$, see Figure 10b. One can see that the sharpness generally increases with the brush parameter ε but saturates at larger ε . The same sharp transition can be seen using the average height of the free end as an indicator. We summarize the properties of the probe chain by presenting the phase diagram in the $(\varepsilon_{probe}, \varepsilon)$ plane, see Figure 11.

To identify the nature of the underlying transitions we present a more detailed study for the case of a relatively strongly attractive substrate, $\varepsilon = 1$, and for the case when the brush chains experience some extra repulsion, $\varepsilon = -1$. We specifically pay attention to two criteria identifying first-order transitions in finite systems: 1) bimodal distributions in the vicinity of the transition point, and 2) the variance of extensive parameters (such as the number of monomers in contact with the substrate) growing $\propto N^2$ as consistent with the system fluctuating between two distinct phases. The changes in the shape of the distribution of the end monomer of the probe chain upon crossing the line separating the probe chain phases are displayed in Figure 12. It is clear that bi-modality

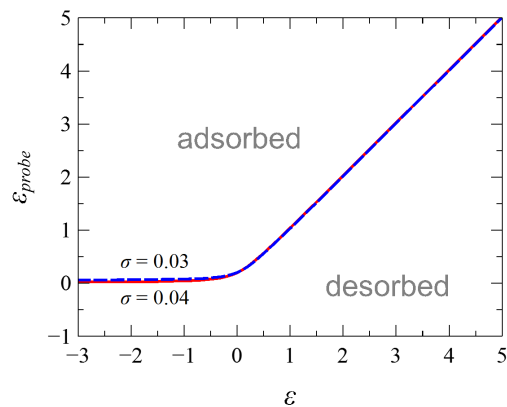


Figure 11. Phase diagram of a probe chain with its own adsorption parameter ε_{probe} in a monodisperse brush with adsorption parameter ε . The probe chain is otherwise the same as the other brush chains.

emerges at the transition in the case of the attractive brush (a), but is absent in the case of extra repulsion (b). We conclude that part of the phase diagram (at large positive ε) can be interpreted as a line of I-order transitions, while the other part (at large negative ε) resembles more a line of II-order continuous transitions.

To verify this conclusion we study finite chain length effects. Figure 13a demonstrates the adsorption curves of the probe chain in the attractive brush with $\varepsilon = 1$ for several values of the brush and probe chain length N (noting that both are the same in the present study). In order to maintain the same relative magnitude of the adsorption effect on the brush, we fix the value of the product $N\sigma = 4$. As the system size N increases, the adsorption curves become steeper although they all intersect at approximately the same point. This behavior is also typical for finite-size effects in I-order transitions [26]. The fluctuations near the transition point become more prominent with increasing N , see Figure 13b, while the position of the peak is unaffected by the system size. The inset demonstrates that the peak values scale as $\text{Var}(m)_{peak} \propto N^2$ confirming the I-order type transition. On the other hand, if the probe chain undergoes the adsorption transition in a brush with extra repulsion, $\varepsilon = -1$, the finite chain length effects look different. The probe chain adsorption curves do not cross for different values of N , see Figure 14a. As for the fluctuations in the number of contacts, the position of the peak shifts to lower values of ε_{probe} with the increase in N , and the maximum variance scales as $\text{Var}(m)_{peak} \propto N^x$ with $x \approx 1.2$, see Figure 14b

We conclude that the phase diagram contains a line of I order transitions $\varepsilon_{probe} = \varepsilon$ for large positive ε . This line eventually degenerates into a line of II-order transitions at negative (and, possibly, very small positive) values of ε where the transition point for the probe chain become almost independent of brush adsorption parameter. From the general mean-field picture of phase transitions one

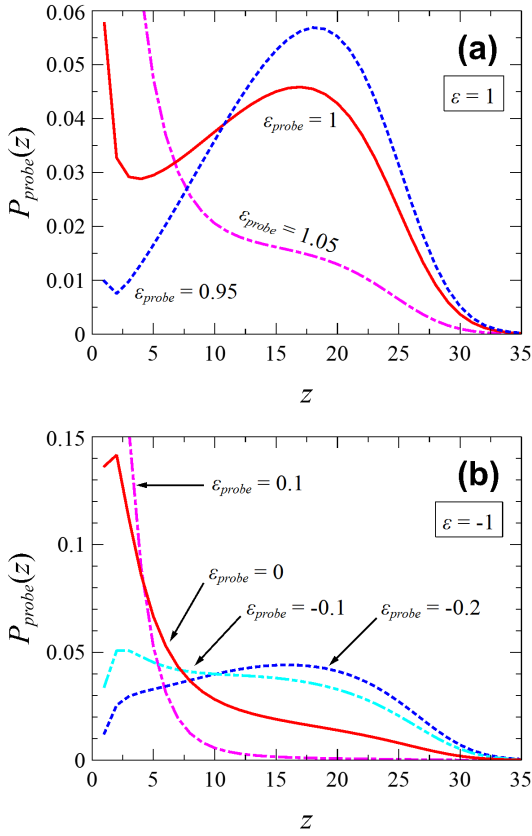


Figure 12. Distributions $P_e(z)$ for the free ends of the probe chain in a monodisperse brush with $N = 100$ and $\sigma = 0.04$ at various the probe chain interaction energy ε_{probe} , as indicated, and brush polymer adsorption energy $\varepsilon = 1$ (a) and -1 (b).

would expect a tricritical point where the lines of the I and II-order transitions are joined together [26, 30]. The exact localization of this point and a detailed study of the tricritical adsorption is outside the scope of the present paper.

Going back to a homogeneous adsorption-active brush with a single adsorption parameter ε we conclude that the brush maintains the density profile exactly corresponding to the line of I-order transitions, and with increasing ε we just move up along that line, never leaving it. This peculiar picture seems to be an inevitable consequence of three conditions: 1) the total number of monomers exceeds the maximum adsorption capacity of the substrate (“hairy” saturation regime) which means that two states must exist; 2) An adsorption scenario whereby a certain fraction of chains is adsorbed thus ensuring phase coexistence at the level of brush chains rather than at the level of monomers; and 3) brush monodispersity which means that all the chains are identical and therefore each chain has to fluctuate strongly between the two phases.

Yet another puzzle appears when we look at the fluctuations of the number of adsorbed monomers, n , per unit area in a homogeneous monodisperse brush. The

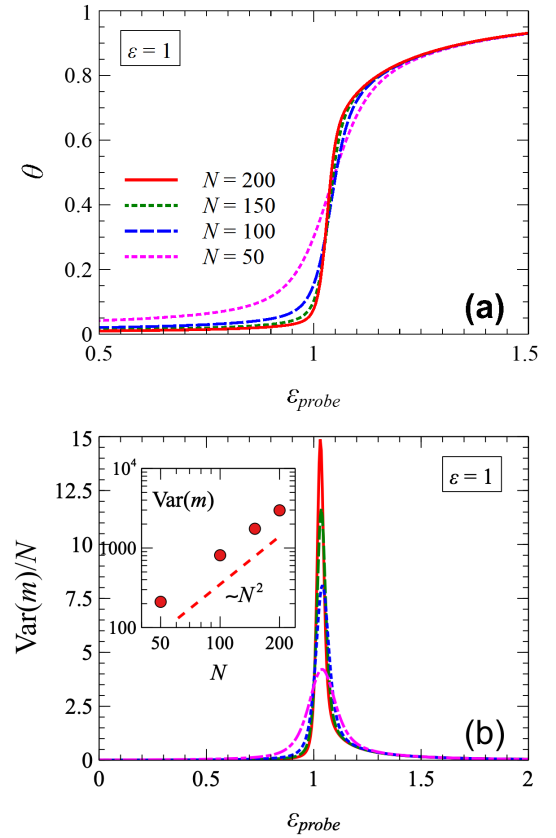


Figure 13. Fraction of adsorbed units in the probe chain (a) and its variance (b) as function of the probe chain interaction energy ε_{probe} at fixed brush chains interaction energy $\varepsilon = 1$.

average number of contacts coincides with the monomer density φ_1 . According to standard thermodynamic formulas, $\varphi_1 = \langle n \rangle = -\frac{\partial F}{\partial \varepsilon}|_{N,\sigma}$ where F is the free energy of the brush per unit area. Mean-square fluctuations in the number of contacts are given by the second derivative, $Var(n) = -\frac{\partial^2 F}{\partial \varepsilon^2}|_{N,\sigma} = \frac{\partial \varphi_1}{\partial \varepsilon}|_{N,\sigma}$ which is the slope of the adsorption curve for a homogeneous brush. It is clear from Figure 4 that the slope is essentially independent of the chain length and does not carry any indication of the large chain fluctuations. We come to a conclusion that although a monodisperse brush is composed of strongly fluctuating chains, these fluctuations must be correlated in such a way that the brush as a whole represents a regular thermodynamic system with a perfectly normal fluctuation behavior. Within the SCF framework it is impossible to verify this picture by following up the correlated changes in the conformations of the neighboring chains, so a complete resolution of this fluctuation paradox would require a MC of MD simulation.

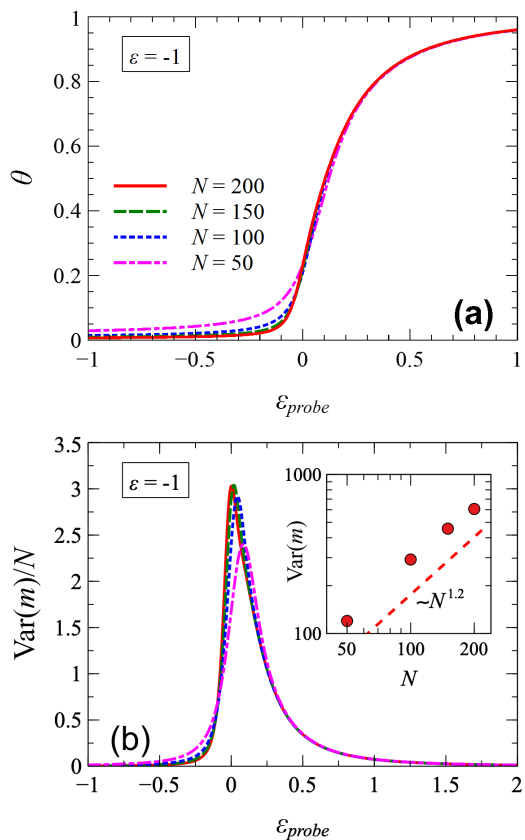


Figure 14. Fraction of adsorbed units in the probe chain (a) and its variance (b) as function of the probe chain interaction energy ϵ_{probe} at fixed brush chains interaction energy $\epsilon = -1$.

VI. DISCUSSION AND SUMMARY

We have demonstrated that a monodisperse brush with a strong enough monomer attraction to the substrate forms a micro-phase separated system with a fraction of chains being in close contact to the surface while the rest of the chains form a residual brush with a reduced effective grafting density. As the adsorption energy ϵ is increased, the fraction of chains in the adsorbed phase initially increases but eventually the system saturates at large values of $\epsilon \gtrsim 3$. Phase coexistence is retained in a very broad range of ϵ and it is impossible to identify a transition point. Indirectly, the adsorption parameter controls the grafting density of the residual brush. Depending on the value of the product σN , in the saturation limit the residual brush may disappear completely or be reduced to isolated mushroom-like tails. We have identified and studied the regime, $\sigma N > 2.5$ in which the residual brush is reasonably well defined for any value of the adsorption energy ϵ .

In some respect, our observations described above are reminiscent of partial wetting [31] as can be observed, e.g., in a gas in contact with an attractive substrate if one approaches the gas/liquid transition: A thin liq-

uid layer forms on the substrate for a wide range of adsorption strengths, similar to the adsorption layer in our adsorption-active brushes. In other respect, however, the situation here is very different from regular wetting: The attractive substrate not only influences the thickness of the wetting layer, but also the properties of the "coexisting" phase, e.g., the effective grafting density of the outer brush. The connectivity of the brush chains transmits a strong coupling between the adsorbed and desorbed layer. It is reflected in strong fluctuations of individual chains between "coexisting" adsorbed desorbed states, which are not sharply defined as the free energy barrier separating them is always small, less than $1kT$ even when the adsorption energy is as large as $\epsilon = 10$. This means that kinetic trapping is most likely absent and the exchange of monomers between phases must be characterized by relatively fast dynamics. Overall, certain features of the behavior of the adsorption-active brush are rather difficult to fit in the conventional framework of the phase transition theory. We have attempted to clarify the situation by introducing the notion of a probe chain and by constructing its phase diagram. This construction answers some questions but raises several others.

A coexistence between stretched and collapsed chains or chain parts has been observed before in polyelectrolyte systems [32]. In the case of polyelectrolyte brushes grafted on oppositely charged substrates the situation is very similar to the one considered here. The charged substrate provides the attractive part of the potential, which is neutralized by the combination of electrostatic screening and steric repulsion due to the dense proximal layer, while the rest of the chains form a residual brush governed by repulsive mean force [33]. Another possibility involves an electrically neutral substrate covered by a polyamphiphilic brush with short chains of one charge and much longer chains of the opposing charge [34]. Here the short blocks create an effective attractive potential localized near the substrate which again competes with a longer-range repulsion. In both cases, a bimodal distribution of global chain characteristics was observed indicating phase coexistence along the second scenario. A more intricate scenario suggesting lateral segregation into collapsed and stretched microphases was observed for weak polyelectrolyte brushes in a poor solvent [35].

In the present study, we have discussed monodisperse polymer brushes only. Polydispersity effects will be investigated in future work. Based on previous results on polydispersity effects in responsive brushes [36], we expect that the main features of the adsorption-active brush reported above will persist, although the fluctuation characteristics of single chains will likely change [37]. Although our discussion was confined to the case of a brush formed by flexible uncharged chains grafted onto a planar substrate and immersed in a good solvent, we believe that the qualitative results concerning the microphase separation and the indirect control of the residual brush by the adsorption parameter are applicable to a much broader class of situations.

The data that support the findings of this study are available from the authors upon reasonable request.

VII. DEDICATION

This paper is dedicated to Tatiana Birshstein who made an outstanding contribution to the contemporary statistical physics of macromolecules and to a great extent promoted the progress in theoretical and experimental polymer science worldwide.

ACKNOWLEDGMENTS

Financially supported by the Russian Foundation for Basic Research through the grant no. 20-53-12020 NNIO.a and by the German Science Foundation through the grant Schm 985/23 is gratefully acknowledged.

Appendix A: The Scheutjens-Fleer self-consistent field method

In the case of a planar brush, we use a one-gradient version of the SF-SCF method, in which the lattice sites are organized in a planar layers, each layer is referred to with a coordinate z normal to the grafting plane. The model is limited to laterally homogeneous systems. In framework of the SF-SCF method, various interactions between the particles in the system are replaced by the mean effective interactions, or the potential $u(z)$. Hence, SCF does not exclude overlapped (not self-avoiding) conformations. In principle, this may result in an underestimation of the entropic cost of collapsing the chains to the attractive surface. However, a detailed study of adsorbed polymer layers has demonstrated an excellent match of the SCF and simulation results [38].

If the potential $u(z)$ is specified, then the statistical weight of a monomer unit is $G(z) = \exp[-u(z)]$. Using the monomer unit's weight, we calculate two statistical weights: the statistical weight $G_t(z, s)$ of a chain with s monomer units tethered at one end at the surface and having its other end in the layer z (the subscript “ t ” means “tethered”) and the the statistical weight $G_f(z, s)$ of a chain with s monomer units having one end pinned in the layer z and the other end free (the subscript “ f ” means “free”). They satisfy the recurrence relations

$$G_{t,f}(z, s+1) = G(z)[\lambda G_{t,f}(z-1, s) + (1-2\lambda)G_{t,f}(z, s) + \lambda G_{t,f}(z, s)] \quad (\text{A1})$$

where λ is the probability that a random walk step connects neighboring layers. On the simple cubic lattice, one has $\lambda = 1/6$. The initial condition for $G_t(z, s)$ and $G_f(z, s)$ are different

$$G_t(z, 1) = \begin{cases} G(z), & z = 1 \\ 0, & z \neq 1 \end{cases} \quad (\text{A2})$$

and

$$G_f(z, N) = \begin{cases} G(z), & z \geq 1 \\ 0, & z < 1 \end{cases} \quad (\text{A3})$$

The recurrence relation (A1) should be modified in the first layer adjacent to the grafting surface: for $z < 1$, $G_{t,f}(z, s) = 0$, hence

$$G_{t,f}(1, s+1) = G(z)[(1-2\lambda)G_{t,f}(1, s) + \lambda G_{t,f}(2, s)]. \quad (\text{A4})$$

This plays the role of the boundary condition at $z = 1$. It is also obvious that for $z > s$, $G_t(z > s, s) = 0$.

By using the set of $G_t(z, s)$ and $G_f(z, s)$ for $1 \leq s \leq N$ one can calculate the polymer volume density profile via the composition law [12]:

$$\varphi(z) = \frac{\sigma}{q} \cdot \frac{\sum_{s=1}^N G_t(z, s) G_f(z, N-s+1)}{G(z)}. \quad (\text{A5})$$

The factor $G(z)$ in the denominator of the rhs of (A5) is used to avoid double counting of the monomer unit in the layer z . The normalization constant is obtained from the condition $\sum_z \varphi(z) = N\sigma$ and includes the partition function of a tethered chain $q = \sum_z G_t(z, N) = G_f(1, N)$.

At each lattice layer, the incompressibility condition is obeyed:

$$\varphi(z) + \varphi_s(z) = 1. \quad (\text{A6})$$

The potential $u(z)$ acting on the monomer units

$$u(z) = -\log[1 - \varphi(z)] - \varepsilon \delta_{z,1} \quad (\text{A7})$$

where the second term is the additional surface attraction energy in the first lattice layer ($z = 1$). ε is the measure of the polymer-surface attraction, $\delta_{i,j}$ is the Kronecker delta.

The system of equations Eqs. (A1), (A4), (A5), and (A7) is solved self-consistently taking into account the incompressibility condition (A6). That is, with an initial guess $u(z)$ one calculates the set of propagators $G_t(z, s)$ and $G_f(z, s)$ [Eqs. (A1) and (A4)], the density profile $\varphi(z)$ [Eq. (A7)] and the new field $u(z)$ [Eq. (A7)]. The procedure is then iteratively repeated until it converges to a fixed point, or the self-consistent solution. Once the solution, i.e the self-consistent potential $u(z)$ is found, this gives access to the density profile, end segment distribution, and can also be used to study the behavior of a probe minority chain inserted into the brush.

- [1] E. P. K. Currie, W. Norde, and M. A. Cohen Stuart. Tethered polymer chains: surface chemistry and their impact on colloidal and surface properties. *Adv Colloid Interface Sci*, 100-102:205–265, 2003.
- [2] N. Ayres. Polymer brushes: Applications in biomaterials and nanotechnology. *Polym. Chem.*, 1:769–777, 2010.
- [3] M. W. Urban. *Handbook of Stimuli-Responsive Materials*. Wiley-VCH Verlag GmbH & Co. KGaA, Weinheim, Germany, 2011.
- [4] B. Jaquet, D. Wei, B. Reck, F. Reinhold, X. Zhang, H. Wu, and M. Morbidelli. Stabilization of polymer colloid dispersions with pH-sensitive poly-acrylic acid brushes. *Colloid Polym. Sci.*, 291(7):1659–1667, 2013.
- [5] M. Motornov, S. Minko, K.-J. Eichhorn, M. Nitschke, F. Simon, and M. Stamm. Reversible tuning of wetting behavior of polymer surface with responsive polymer brushes. *Langmuir*, 19(19):8077–8085, 2003.
- [6] M. A. Cohen Stuart, W. T. S. Huck, J. Genzer, M. Müller, C. Ober, M. Stamm, G. B. Sukhorukov, I. Szleifer, V. V. Tsukruk, M. Urban, F. Winnik, S. Zauscher, I. Luzinov, and S. Minko. Emerging applications of stimuli-responsive polymer materials. *Nat. Mater.*, 9(2):101–113, 2010.
- [7] S. Qi, L. I. Klushin, A. M. Skvortsov, A. A. Polotsky, and F. Schmid. Stimuli-responsive brushes with active minority components: Monte Carlo study and analytical theory. *Macromolecules*, 48(11):3775–3787, 2015.
- [8] T. Chen, R. Ferris, J. Zhang, R. Ducker, and S. Zauscher. Stimulus-responsive polymer brushes on surfaces: Transduction mechanisms and applications. *Prog. Polym. Sci.*, 35(1-2):94 – 112, 2010. Special Issue on Stimuli-Responsive Materials.
- [9] S. Gupta, M. Agrawal, P. Uhlmann, F. Simon, U. Oertel, and M. Stamm. Gold nanoparticles immobilized on stimuli responsive polymer brushes as nanosensors. *Macromolecules*, 41(21):8152–8158, 2008.
- [10] H. Merlitz, G.-L. He, J.-U. Sommer, and Ch.-X. Wu. Reversibly Switchable Polymer Brushes with Hydrophobic/Hydrophilic Behavior: A Langevin Dynamics Study. *Macromolecules*, 42(1):445–451, 2009.
- [11] H. Pasch and B. Trathnigg. Multidimensional HPLC of polymers. 2013.
- [12] G. J. Fleer, M. A. Cohen Stuart, J. M. H. M. Scheutjens, T. Cosgrove, and B. Vincent. *Polymers at Interfaces*. Chapman and Hall, London, 1993.
- [13] A. Halperin. On Polymer Brushes and Blobology: An Introduction. In Y. Rabin and R. Bruinsma, editors, *Soft order in Physical Systems. NATO ASI Series*, volume 323, pages 33–56. Springer, Berlin Heidelberg, 1994.
- [14] M. Rubinstein and R. H. Colby. *Polymer Physics*. Oxford University Press, Oxford, 2003.
- [15] S. T. Milner, T. A. Witten, and M. E. Cates. Theory of the grafted polymer brush. *Macromolecules*, 21(8):2610–2619, 1988.
- [16] Ye. B. Zhulina, V.A. Pryamitsyn, and O. V. Borisov. Structure and conformational transitions in grafted polymer chain layers. a new theory. *Polymer Science U.S.S.R.*, 31(1):205 – 216, 1989.
- [17] P.G. De Gennes. Scaling theory of polymer adsorption. *J. Phys. France*, 37(12):1445–1452, 1976.
- [18] P. G. De Gennes. Polymer solutions near an interface. adsorption and depletion layers. *Macromolecules*, 14(6):1637–1644, 1981.
- [19] E. Bouchaud and M. Daoud. Polymer adsorption: concentration effects. *J. Phys. France*, 48(11):1991–2000, 1987.
- [20] R. Descas, J.-U. Sommer, and A. Blumen. Concentration and saturation effects of tethered polymer chains on adsorbing surfaces. *The Journal of Chemical Physics*, 125(21):214702, 2006.
- [21] R. Descas, J.-U. Sommer, and A. Blumen. Static and dynamic properties of tethered chains at adsorbing surfaces: A Monte Carlo study. *The Journal of Chemical Physics*, 120(18):8831–8840, 2004.
- [22] P. G. de Gennes and P. Pincus. Scaling theory of polymer adsorption: Proximal exponent. *J. Physique - Lettres*, 44:L-241–L-246, 1983.
- [23] P. Grassberger. Simulations of grafted polymers in a good solvent. *J. Phys. A: Math. Gen.*, 38:323, 2005.
- [24] L. I. Klushin, A. A. Polotsky, H.-P. Hsu, D. A. Markelov, K. Binder, and A. M. Skvortsov. Adsorption of a single polymer chain on a surface: Effects of the potential range. *Phys. Rev. E*, 87:022604, Feb 2013.
- [25] S. Zhang, S. Qi, L. I. Klushin, A. M. Skvortsov, D. Yan, and F. Schmid. Phase transitions in single macromolecules: Loop-stretch transition versus loop adsorption transition in end-grafted polymer chains. *J. Chem. Phys.*, 148:044903, 2018.
- [26] L. I. Klushin and A. M. Skvortsov. Unconventional phase transitions in a constrained single polymer chain. *J. Phys. A: Math. Theor.*, 44(47):473001, 2011.
- [27] E. Eisenriegler, K. Kremer, and K. Binder. Adsorption of polymer chains at surfaces: Scaling and monte carlo analyses. *The Journal of Chemical Physics*, 77(12):6296–6320, 1982.
- [28] A. M. Skvortsov, A. A. Gorbunov, F. A. M. Leermakers, and G. J. Fleer. Long minority chains in a polymer brush: A first-order adsorption transition. *Macromolecules*, 32(6):2004–2015, 1999.
- [29] L. I. Klushin, A. M. Skvortsov, A. A. Polotsky, S. Qi, and F. Schmid. Sharp and fast: Sensors and switches based on polymer brushes with adsorption-active minority chains. *Phys. Rev. Lett.*, 113:068303, Aug 2014.
- [30] P. M. Chaikin and T. C. Lubensky. *Principles of Condensed Matter Physics*. Cambridge University Press, 1995.
- [31] P. G. de Gennes. Wetting: Statics and dynamics. *Rev. Mod. Physics*, 57:827–863, 1985.
- [32] Q. Wang. Modelling Layer-by-Layer Assembly of Flexible Polyelectrolytes. *J. Phys. Chem. B*, 110:5825–5828, 2006.
- [33] H. Merlitz, C. Li, C. Wu, and J.-U. Sommer. Polyelectrolyte brushes in external fields: molecular dynamics simulations and mean-field theory. *Soft Matter*, 11:5688–5696, 2015.
- [34] N. P. Shusharina and P. Linse. Oppositely charged polyelectrolytes grafted onto planar surface: Mean-field lattice theory. *Eur. Phys. J. E*, 6(2):147–155, 2001.
- [35] M. Tagliacuzzi, M. Olvera de la Cruz, and I. Szleifer. Self-organization of grafted polyelectrolyte layers via the coupling of chemical equilibrium and physical interactions. *PNAS, Proc. Natl. Acad. Sci. USA*, 107(12):5300–5305, 2010.

- [36] S. Qi, L. I. Klushin, A. M. Skvortsov, M. Liu, J. Zhou, and F. Schmid. Tuning transition properties of stimuli-responsive brushes by polydispersity. *Adv. Functional Materials*, 28:1800745, 2018.
- [37] S. Qi, L. I. Klushin, A. M. Skvortsov, and F. Schmid. Polydisperse polymer brush: Internal structure, critical behavior, and interaction with flow. *Macromolecules*, 49:9665–9683, 2016.
- [38] G. J. Fleer and F. A. M. Leermakers. Statistical thermodynamics of polymer layers. *Curr. Opin. Coll. Interf. Sci.*, 2(3):308 – 314, 1997.